Vibrationally State-Selective Spin−Orbit Transfer with Strong Nonresonant Pulses

Jesús González-Vázquez,[†] Ignacio R. Sola,*[,†] Jesus Santamaria,[†] and Vladimir S. Malinovsky[‡]

Departamento de Química Física, Universidad Complutense, 28040 Madrid, Spain, and MagiQ Technologies, Inc., 171 Madison Avenue, Suite 1300, New York, New York 10016

Received: October 17, 2006; In Final Form: February 2, 2007

By dynamic Stark shift using strong nonresonant pulses, we show that it is in principle possible to prepare arbitrary superposition states of mixed multiplicity. By a proper choice of parameters, the transfer of population is shown to follow the Rabi formula, where the initial and target states are now vibrational states of two light-induced molecular potentials of different multiplicity. Starting from nonstationary wave packets, the spin transfer can proceed via parallel transfer using a single pulse or by sequential transfer using a pulse sequence. A simple model is proposed to analyze the properties of both schemes and the feasibility of their experimental implementation for spin−orbit transitions in Rb_2.

1. Introduction

With a proper "photon environment", many simple systems can reproduce interesting and often unexpected functional behaviors. Quantum control with laser fields is thus becoming a viable alternative approach to Hamiltonian engineering of quantum systems or quantum materials.[1,2] Because the control is exerted in the time domain (in a broad sense, the control knob is the external time-dependent field), it is important to understand how and when can it affect parts of the Hamiltonian that cannot be coupled via dipole moment, to any order of the field, at least in the so-called diabatic representation.[3] Controlling the transition between two states that are not coupled by the field is usually called the control of dark transitions. In this work, we focus on one such dark transition: the spin−orbit coupling. We analyze the role of dynamic Stark shifts induced by strong nonresonant fields, and we propose several strategies for achieving vibrationally selective population transfer between singlet and triplet quantum states. The general mechanism, however, is generally valid for controlling dipole-forbidden transitions and could be used in wider contexts.

Although the spin−orbit coupling is usually treated as a weak perturbation important mainly for high-resolution spectroscopy,[3] it has also significant implications in the predissociation dynamics of molecules,[4,5] especially if heavy atoms are involved, and in the rate of relaxation mechanisms.[6] More importantly for our study, it has immediate use in solid or molecular magnetism. The implementation of efficient and fast optical spin switches, with potential applications in molecular memories, for example, would imply a technological breakthrough in the field of quantum information.[7,8] To that end, it is particularly important to manipulate quantum superposition states of different multiplicity and thus selectively transfer population between specific quantum states of different spin. Until now, only a few schemes have been proposed to control spin transitions using strong laser pulses. Most notably, Hübner et al. have proposed and numerically tested the possibility of inducing full optical spin switches by ultrashort π pulses,[9−14] and Korolkov et al. induced the spin switching by coherent control techniques.[15,16] In these studies, the performance of the schemes was not analyzed for initial nonstationary quantum superpositions, which are typically the required states for driving quantum information. On the other hand, Sussman et al.[17,18] and Chan et al.[19] controlled the rate of dissociation reactions involving channels with spin−orbit curve-crossing potentials.

In recent work of our group, we have proposed a scheme to control the spin−orbit coupling.[20−22] The underlying mechanism of the scheme implied controlling the energy difference between the states of different spin, which are coupled by spin−orbit interaction, in order to enhance or inhibit the flow of population. The energy control on the dark transition was achieved by nonresonant dynamic Stark shift, as in refs 17,18,23, among the set of states that are coupled by the laser field. We shall also use the name nonresonant dynamic Stark effect (NRDSE), proposed by Sussman et al.,[17] to refer to the laser scheme.

We have tested the NRDSE in two different regimes. In the weak-field limit, we have shown how it is possible to prepare superposition states of arbitrary spin components.[20] The scheme could only work for weak spin−orbit coupling in molecules with a low density of states, typically using long coherent pulses. In the opposite limit,[21,22] using the Rb_2 as a test system, we have shown that it is possible to stop or freeze the flow of population between two electronic states of different multiplicity that are strongly coupled.

In this work, we consider again a simple test system with strong spin−orbit couplings. We will show that it is in principle possible to use the same basic ideas of controlling the dynamic Stark effect in order to enhance the transfer of population between states of different spin multiplicity with quantum state selectivity. Furthermore, we will show that it is possible to prepare arbitrary mixed-spin superposition states starting from nonstationary superposition states. In certain regimes, one is able to generalize the famous Rabi formula[24] by which the population inversion is achieved by resonance (induced by field amplitude) and time (laser duration) control. The spin switch can be induced with a single pulse, in parallel for all the initial wave packet components, or sequentially, by using a pulse sequence. However, the laser requirements for state-selective

* To whom correspondence should be addressed. E-mail: ignacio@tchiko.quim.ucm.es.
[†] Departamento de Química Física, Universidad Complutense.
[‡] MagiQ Technologies, Inc.

10.1021/jp066825y CCC: $37.00
Published on Web 03/20/2007

spin transfer are more demanding than in previous studies[21,22] and will be harder to meet in actual experiments.

The organization of the paper is the following: In Section 2, we describe the NRDSE process and the required conditions for the laser-induced state-selective spin transfer. In Section 3, we propose the simplest molecular scenario where this spin switch can take place, and we propose three different strategies to implement the NRDSE, the vibrational state-to-state transfer, the parallel transfer of all the vibrational components of an initial singlet wave packet, and the sequential transfer of part of the vibrational components of an initial singlet wave packet. In Section 4, we suggest some possible applications of the scheme for certain singlet−triplet "dark" transitions in Rb_2. Finally, Section 5 is the conclusion.

2. State-Selective Spin Transfer under a Strong Field

In this section, we will set up the simplest model that takes into account the effects of a relatively strong nonresonant field acting on a diatomic molecule in order to induce selective vibronic population transfer between a given vibrational level in a singlet electronic state, $^1\varphi_i(x)$, and a suitably chosen vibrational level in an energetically close triplet electronic state, $^3\varphi_j(x)$. In the absence of the field, the population transfer between the two levels follows the well-known Rabi formula.[24] Assuming that a single constant field ϵ is continuously acting on the system, the straightforward extension of the Rabi formula gives the time-dependent final population as:

$$P_j(t;\epsilon) = \frac{4V_{ij}(\epsilon)^2}{4V_{ij}(\epsilon)^2 + \Delta E_{ij}(\epsilon)^2} \sin^2\left(\frac{t}{2}\sqrt{\Delta E_{ij}(\epsilon)^2 + 4V_{ij}(\epsilon)^2}\right) \tag{1}$$

where $\Delta E_{ij}(\epsilon)$ is the energy difference between $^3\varphi_j(x;\epsilon)$ and $^1\varphi_i(x;\epsilon)$, and $V_{ij}(\epsilon) = \langle ^3\varphi_j(\epsilon)|V_{SO}|^1\varphi_i(\epsilon)\rangle$ is the state-to-state spin−orbit coupling. Assuming second-order perturbation theory for the field interaction, both magnitudes depend on the nonresonant field due to the Stark shifts ($\Delta E_{ij}(\epsilon)$ on second order and $V_{ij}(\epsilon)$ on fourth order). This stems directly from the polarizability effects in the rotating-wave approximation (RWA) Hamiltonian:[17,21]

$$\mathscr{H} = \begin{pmatrix} T + V_S(x) - \alpha_S(x)\epsilon(t)^2/4\Delta_S & V_{SO} \\ V_{SO} & T + V_T(x) - \alpha_T(x)\epsilon(t)^2/4\Delta_T \end{pmatrix} \tag{2}$$

where $\alpha_S(x)$ and $\alpha_T(x)$ are the singlet and triple polarizabilities, T the kinetic energy operator, and Δ_S and Δ_T the singlet and triplet detunings due to the nonresonant nature of the interaction. From the vibrational levels and eigenfunctions of the Stark-shifted potentials, $V_S(x) - \alpha_S(x)\epsilon(t)^2/4\Delta_S$ and $V_T(x) - \alpha_T(x)\epsilon(t)^2/4\Delta_T$, one can easily calculate the field dependence of the energy difference and the coupling:[21]

$$\Delta E_{ij}(\epsilon) = \Delta E_{ij}(0) + \frac{1}{4}\left(\frac{\alpha_S(i,i)}{\Delta_S} - \frac{\alpha_T(j,j)}{\Delta_T}\right)\epsilon^2 \tag{3}$$

where $\Delta E_{ij}(0)$ is the energy difference in the absence of the field and we define $\alpha_S(i,i) = \langle ^1\varphi_i|\alpha_S|^1\varphi_i\rangle$ and similarly $\alpha_T(j,j) = \langle ^3\varphi_j|\alpha_T|^3\varphi_j\rangle$. The dependence of $V_{ij}(\epsilon)$ with the field is via the fourth-order perturbation expression of the wave functions $^1\varphi_i(x;\epsilon)$ and $^3\varphi_j(x;\epsilon)$. This dependence is more complex, and we shall not attempt to give the expression here because, as we will show later, the coupling is in fact independent of the field if one calculates it for all orders of the perturbation in the adiabatic limit. For strong fields, the later is a much better approximation than fourth-order perturbation theory.

By using eq 1, it is easy to understand how the field can be used to control the flow of population. If initially $|\Delta E_{ij}(0)| \gg |V_{ij}|$ in the absence of the laser, the spin−orbit coupling can only account for a small perturbation in the population dynamics, thus one must choose ϵ to make $\Delta E_{ij}(\epsilon) \approx 0$. Full population inversion will then occur in a time $\tau = \pi/2|V_{ij}|$, after which the pulse should be turned off so that the population cannot recross back to the initial state. Following eq 3, the system will be controllable as long as $\alpha_T(j,j)/\Delta_T \neq \alpha_S(i,i)/\Delta_S$, and the Hamiltonian is not symmetric with respect to the dynamical polarizabilities. Additionally, eq 1 is only valid if the coupling V_{ij} is smaller than the vibrational energy spacing between adjacent vibrational levels in the singlet and triplet potentials; otherwise, the population will flow to a manifold of closely spaced triplet and singlet vibrational levels, losing the quantum selectivity. However, whereas the initial state, $^1\varphi_i(x)$, is given, $^3\varphi_j(x)$ is selected by a proper choice of the field intensity ϵ, such that the energy difference is zero or close to zero. Therefore, the final state can be chosen such that the coupling with all the closest triplet vibrational levels is weak enough, validating the simple picture given by eq 1. It is interesting to observe that the state selectivity in our problem is achieved by field intensity requirements, not resonant frequency conditions. The carrier frequency of the pulse enters, however, as a control knob in a more subtle way from the detunings Δ_S and Δ_T of eq 3.

In this work, we control the dynamics of a molecule with large spin−orbit couplings. The selective transfer will require finding appropriate states of the Hamiltonian for the target states, where the population is excited, as discussed previously. Therefore, strong pulses will be needed to shift the target states into resonance with the initial states. To reduce the intensity demands of the method, instead of working in very off-resonant conditions, the Stark shift will be induced mainly by a single electronic state to which $V_T(x)$ or $V_S(x)$ are strongly coupled by a suitable choice of the laser frequency, as demonstrated by Frohnmeyer et al.[25] Then the description in eq 2 in terms of the polarizabilities is not valid. For near-resonant excitations (or, in fact, whenever the laser amplitudes involved are as large as the detunings), absorption can compete with Raman processes, and moreover, photon-induced crossings or near-crossings can not only shift but also reshape and distort the potentials $V_S(x)$ and $V_T(x)$ in eq 2. It is then more accurate to use as a first approximation a minimal description of the dynamics based on three electronic potentials: the initial singlet and the target triplet potentials and a third electronic potential, which is dipole-coupled to either the initial singlet or the target triplet and which induces the desired Stark shift. We shall call it $V_e(x)$. Typically, it will be a triplet potential chosen to be relatively far from other electronic singlet states so that one can minimize the laser disturbance to the initially populated singlet wave function. This model can be conveniently generalized by including more singlet and triplet electronic states. In the RWA, the simplest Hamiltonian for the spin-coupling control under the influence of moderately intense fields is therefore:

$$\mathscr{H} = \begin{pmatrix} T + V_S(x) & V_{SO} & 0 \\ V_{SO} & T + V_T(x) & -\mu\epsilon(t)/2 \\ 0 & -\mu\epsilon(t)/2 & T + V_e(x) - \hbar\omega \end{pmatrix} \tag{4}$$

where μ is the dipole moment between $V_T(x)$ and $V_e(x)$ and ω is the laser carrier frequency. By this simple model, only one

potential, $V_e(x)$, induces the Stark effect over $V_T(x)$, while $V_S(x)$ is neither shifted nor distorted by the field.

It is interesting to consider if (and how) the simple state-selective transfer given by the Rabi formula (eq 1) emerges in the frame of the more complex Hamiltonian in eq 4. The relation can be established in the representation of dressed or light-induced potentials[26] (LIPs). By first dividing the Hamiltonian matrix in three components, $\mathscr{H} = \mathscr{V} + \mathscr{V}'_{SO} + \mathscr{T}$, where $\mathscr{V}$ includes the original diabatic potentials (V_S, V_T, and V_e) and the laser dipole-coupling ($-\mu\epsilon$), $\mathscr{V}'_{SO}$ is the spin−orbit matrix, and $\mathscr{T}$ is the kinetic part; and second, by diagonalizing $\mathscr{V}$, one obtains the LIP representation, $\mathscr{U} = \mathscr{R}^\dagger \mathscr{V} \mathscr{R}$. In this representation, the Hamiltonian is

$$\mathscr{H}_{ad} = \mathscr{U} + \mathscr{R}^\dagger(\mathscr{V}'_{SO})\mathscr{R} + \mathscr{R}^\dagger \mathscr{T} \mathscr{R} \approx \mathscr{U} + \mathscr{U}_{SO} + \mathscr{T} \quad (5)$$

where $\mathscr{U}_{SO} = \mathscr{R}^\dagger(\mathscr{V}'_{SO})\mathscr{R}$, which in principle is not diagonal. In eq 5, we have assumed that the kinetic energy is barely changed by the similarity transformation, but this approximation can be removed. Now, assuming that the excitation is "adiabatic", as $\epsilon(t)$ is turned on, the populations in the diabatic states $\mathscr{V}$ will adiabatically correlate with populations in the corresponding adiabatic states in $\mathscr{U}$: thus, $^1\varphi_i(x)$ correlates with the corresponding vibrational eigenfunction of the LIP $U_S(x,\epsilon)$ created by the laser, which we call $^1\Phi_i(x,\epsilon)$. In fact, in the Hamiltonian of eq 4, $^1\Phi_i(x,\epsilon) \equiv {}^1\varphi_i(x)$ because the laser does not affect singlet states. Similarly, the target state will correspond to one vibrational eigenfunction of the triplet LIP that correlates with $V_T(x)$, $U_T(x,\epsilon)$, which will mix some contribution of $V_e(x)$ and which we call $^3\Phi_j(x,\epsilon)$. As long as the remaining vibrational states of the LIPs do not interfere in the resonant state-to-state coupling, the generalized Rabi equation (eq 1) will be valid, where $\Delta E_{ij}(\epsilon)$ is now the energy difference between $^1\varphi_i(x)$ (or $^1\Phi_i(x,\epsilon)$ in general) and $^3\Phi_j(x,\epsilon)$. This is the energy difference that must be suppressed in the adiabatic representation so that the spin-transfer efficiency is maximal. On the other hand, we obtain[27] $U_{ij} \equiv \langle {}^3\Phi_j | \mathscr{U}_{SO} | {}^1\Phi_i \rangle = \langle {}^3\Phi_j \mathscr{R}^\dagger | \mathscr{R} \mathscr{V}'_{SO} \mathscr{R}^\dagger | \mathscr{R}\, {}^1\Phi_i \rangle \approx \langle {}^3\varphi_j | V_{SO} | {}^1\varphi_i \rangle \equiv V_{ij}$, which shows that the coupling is independent of the field. Moreover, because we have assumed V_{SO} to be coordinate-independent, then $|V_{ij}| = V_{SO}F_{ij}$, where $F_{ji} = |\langle {}^3\varphi_j | {}^1\varphi_i \rangle|$ is the absolute value of the Franck−Condon amplitude of the chosen transition. Because the couplings in the adiabatic and diabatic representations are equivalent, we can use the Franck−Condon amplitudes in the diabatic or molecular potentials to determine the required pulse durations ($\tau = \pi/2|V_{ij}|$) that maximize the efficiency of the transfer. The pulse duration will be used as the main criteria to select the most convenient target states in the selective transfer, namely those states with smaller τ but such that the coupling with the adjacent states is smaller than their energy difference.

3. Numerical Results for a Test Model

In this section, we shall explain how the proposed scheme can be used to induce selective population transfer between an initial wave function in $V_S(x)$ (either a single eigenstate or a wave packet) and a state-selective target wave function in$V_T(x)$. To test the scheme, we will build a general and simple model based on the energetics of the well-known Rb_2 molecule.[4,5,28,29] Because the purpose of this work is general, we shall model the system is terms of very few parameters. The model is first generalized by using Morse potentials. The parameters of the singlet $V_S(x) \equiv f_M(x) = D\cdot(1 - \exp[\beta(x - x_0)]^2$ are chosen to fit the $D^1\Pi_u$ electronic state obtained from ab initio calculations by Park et al.[29] The triplet is constructed by simply shifting and displacing the previous Morse function so that the energetics resembles that of the $1^3\Delta_u$ state, $V_T(x) = f_M(x - d) + \Delta_1$. $1^3\Delta_u$ is relatively close to $D^1\Pi_u$ and thus can serve as an appropriate target triplet. The spin−orbit coupling between both electronic states is estimated as[28] $V_{SO} \approx 10$ cm^{-1}, which we assume coordinate-independent. Finally, $V_e(x)$ is constructed as $V_T(x)$ shifted in energy so that $V_e(x) - \hbar\omega = f_M(x - d) + \Delta_2$. By this choice, the coupling does not distort the shape of the triplet LIPs, that is, the Stark shift only causes energy shifting of the overall potential energy in $V_T(x)$. In atomic units, the parameters are: $D = 8.75 \times 10^{-3}$, $\beta = 0.323$, $x_0 = 8.80$, $d = 0.4$, $\Delta_1 = 0.007$, and $\Delta_2 = 0.018$. The resultant potentials are shown in Figure 1. Despite the simplicity of this model, we shall later see that it can conveniently represent different realistic molecular scenarios.

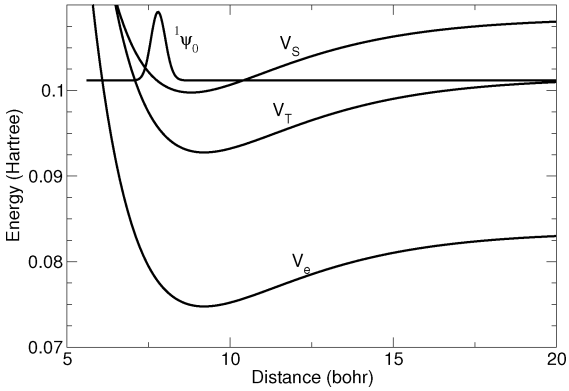

Figure 1. Potential energy curves for the simplest molecular model used in the spin-switch problem.

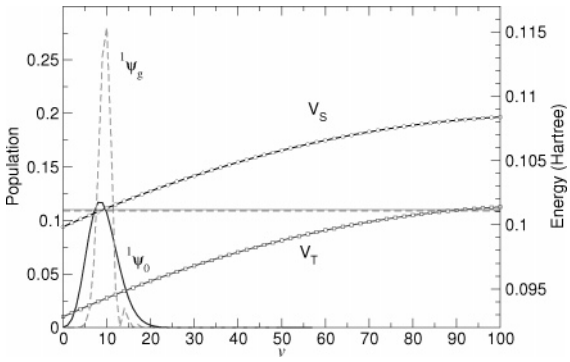

Figure 2. Initial states and electronic potentials in the energy representation. In the left-side scale, we show the populations as a function of the vibrational quanta (υ) of the ground wave function $^1\psi_0$ (solid line) and of the initial state $^1\psi_g$ (dashed line). In the right-side scale, we show the average energy of the wave functions (it is the same for both cases). For reference, we also show the energy of the vibrational eigenstates of the singlet $V_S(x)$ and triplet $V_T(x)$ potentials so that one can observe the energy difference that the field must provide to bring the states into resonance.

To simulate the dynamics of the spin−orbit coupling, we solve the time-dependent Schrödinger equation (TDSE) $(\partial/\partial t)\Psi = -(i/\hbar)\mathscr{H}\Psi$, where Ψ is the wave function of the system and H is the Hamiltonian in eq 4, using the split-operator method.[30] The initial state will be chosen either as the ground vibrational eigenstate of $V_S(x)$, $^1\varphi_0(x)$, or a wave packet, $^1\psi_g(x)$. This wave packet is constructed by minimizing the energy spread of the initial ground vibrational state of the molecule, $^1\psi_0(x)$ (the $\upsilon = 0$ eigenstate of the ground potential), vertically excited in$V_S(x)$, while keeping the same average energy. Figure 2 shows graphically the difference between the true ground vibrational state and our chosen initial wave packet. $^1\psi_g(x)$ was chosen for

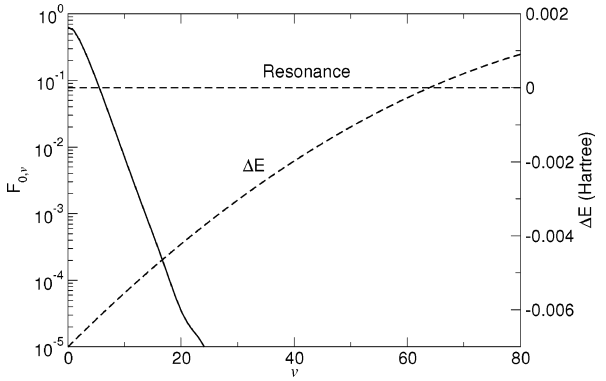

Figure 3. Franck−Condon amplitudes (solid line, left-side scale) and energy difference (dashed line, right-side scale) between the initial wave function and vibrational eigenstates of the triplet potential. In the absence of the field, $^1\varphi_0(x)$ is in resonance ($\Delta E = 0$) with the $v = 64$ vibrational state of $V_T(x)$, shown by the horizontal line.

illustration purposes: it is simpler to analyze the selective transfer (the quantum "information" content) for a superposition of a few eigenstates instead of a wave packet very spread in energy. However, in principle, the scheme can be equally applied to any initial wave function.

We will illustrate the application of the scheme to three different cases. First, we will show how a single eigenstate [$^1\varphi_0(x)$] is transferred to a single eigenstate in $V_T(x)$. We will explain how to properly select the target state. Second, we will consider the *parallel transfer* of the wave packet to the triplet potential, and we will discuss under what conditions this is possible. Finally, we will analyze the *sequential transfer* of each wave packet component into a different target component constructing the target wave packet.

3.1. Single Eigenfunction Switch. Consider that we want to transfer an initial vibrational eigenstate in the singlet, $^1\varphi_0(x)$, to a single quantum state in the triplet. The mechanism of the method implies using a pulse of the precise amplitude such that, by Stark shift, the initial and final states are degenerate, maximizing the transfer probability. The pulse must be switched on during a time

$$\tau = \frac{\pi}{2V_{SO}F_{0v}} \tag{6}$$

where F_{0v} is the absolute value of the Franck−Condon amplitude for the $^1\varphi_0(x) \rightarrow {}^3\varphi_v(x)$ transition. The first question that we address is the following: If the final quantum state is not predetermined, how do we choose the most suitable target state?

Figure 3 shows the energy difference between $^1\varphi_0(x)$ and vibrational eigenfunctions of $V_T(x)$. In the absence of the field, the initial state is on resonance with $^3\varphi_{64}(x)$. However, the Franck−Condon amplitude is practically zero (below numerical precision, so that $V_{0,64} < 10^{-12}$, $\tau > 1$ s). Therefore, no singlet−triplet population transfer can be observed. Because the switching time is inversely proportional to F_{0v}, one needs a high F_{0v} (shown on the left-hand-side scale of Figure 3), yet such that the coupling $V_{0v} = F_{0v}V_{SO}$ is smaller than the vibrational energy spacing with adjacent states, $V_{0v} \ll \Delta\omega$, allowing the transfer to be selective. This can be achieved, for instance, choosing $^3\varphi_4(x)$ ($v = 4$) as the target state. Then $F_{0,4} = 0.17$, $V_{0,4} = 8.5 \times 10^{-6}$ E_h (hartree) and $\tau = 4.7$ ps, while the energy difference between $^3\varphi_4(x)$ and $^3\varphi_3(x)$ ($\Delta\omega \equiv {}^3\Delta E_{3,4}$), or between $^3\varphi_4(x)$ and $^3\varphi_5(x)$ ($\Delta\omega \equiv {}^3\Delta E_{4,5}$) is 1.48×10^{-4} and 1.46×10^{-4} E_h respectively, much larger than the coupling.

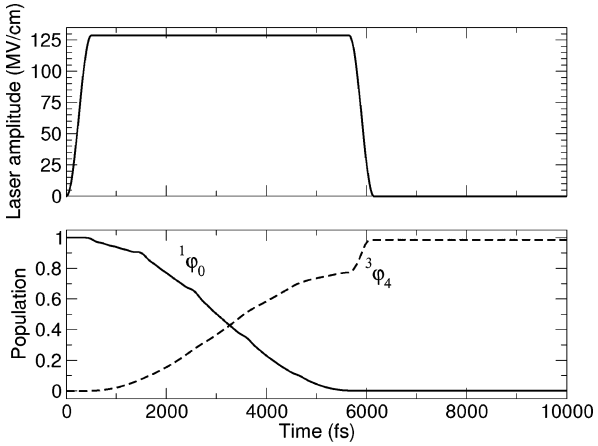

Figure 4. Vibrationally state selective spin-switch between the initial wave function in $V_S(x)$ and $v = 4$ in $V_T(x)$, together with the laser pulse needed for the population transfer.

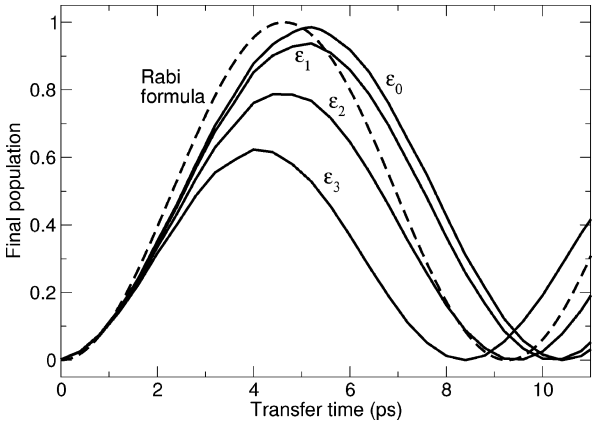

Figure 5. Final population transferred from $^1\varphi_0(x)$ to $^3\varphi_3(x)$ as a function of the laser duration for different pulse amplitudes (all in atomic units): $\epsilon_0 = 2.502 \times 10^{-2}$, $\epsilon_1 = 2.501 \times 10^{-2}$, $\epsilon_2 = 2.500 \times 10^{-2}$, $\epsilon_3 = 2.499 \times 10^{-2}$. (To these amplitudes correspond approximately the following peak intensities in TW/cm^2: 21.91, 21.89, 21.875, and 21.86, respectively.) The dynamics follows closely the Rabi formula, obtained from eq 1 with $\Delta E(\epsilon) = 0$ and $V_{ij}(\epsilon) = V_{04}$.

In Figure 4, we show how the optimal laser drives the population switch between $^1\varphi_0(x)$ and $^3\varphi_4(x)$. We have chosen a field with constant amplitude $\epsilon = 128.6$ MV/cm (implying a peak intensity of ~21.8 TW/cm^2) and 5.1 ps duration, with sine square turn on/off of 0.5 ps duration. Because the laser is strong, the dynamics excites the population to the adiabatic state $^3\Phi_4(x;\epsilon)$, which is a mixture of $^3\varphi_4(x)$ and the fifth eigenstate of $V_e(x)$, $^3\chi_4(x)$. Only when the laser is off, $^3\Phi_4(x;\epsilon)$ adiabatically correlates with $^3\varphi_4(x)$ alone. This explains the fast rise of the population at final times of the switching.

Although the dynamics is driven by strong fields, eq 1 applies reasonably well. In Figure 5, we show how the final population changes as a function of the time duration of the field, τ. Practically, only the initial and target levels participate in the overall transfer. However, the optimal parameters are not exactly those estimated from $V_{0,4}$. Although for $\tau = 4.7$ ps the population transfer is approximately 96%, the maximum value is obtained with almost a 10% increase in τ, which corresponds to an effective Rabi frequency that is nearly 10% smaller than that predicted before.

As explained, the laser amplitude takes the role of selecting the target state, much as the role of frequency in high-resolution spectroscopy. In Figure 6, we analyze the effect of amplitude variations on the selectivity of the transfer. As the figure shows,

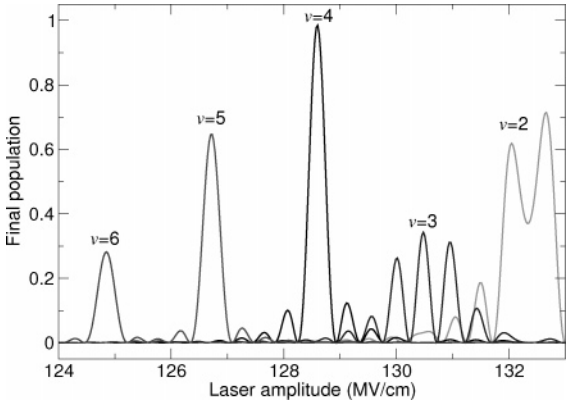

Figure 6. Final population transferred as a function of the laser amplitude. Other pulse parameters are optimized to target $\nu = 4$. The different curves show the excitation of different vibrational quantum states in $V_T(x)$.

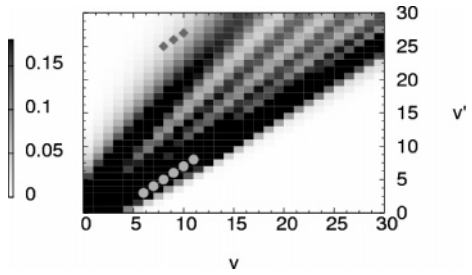

Figure 7. Map of the Franck−Condon amplitudes between vibrational eigenfunctions of $V_S(x)$ (denoted by υ) and $V_T(x)$ (denoted by υ'). The circles show the best choice for parallel state-to-state transfer of all ${}^1\varphi_\upsilon(x)$ components, whereas the diamonds show a better choice for sequential state-to-state transfer of a set of selected initial components.

the resonance between the initial and target state is very sensitive to the field amplitude. Variations of more than 0.1% in the field greatly reduce the efficiency of the transfer. Therefore, for small fluctuations of the field, the optimal time duration should increase because only when the field is very close to the required value will it drive the transition. Unfortunately, if the field amplitude changes over 2% of the optimal value, the population is switched to a different target state (${}^3\varphi_5(x)$ or ${}^3\varphi_3(x)$ for a positive or negative fluctuation, respectively). This poses very demanding experimental conditions on the laser stabilization.[31]

3.2. Parallel Transfer. We will consider now the spin switch of an initial singlet superposition state, $\psi_g(x)$, into the triplet potential, $V_T(x)$. In this case, the dynamics involves the selective transfer of each eigenstate component of the initial wave function (or a set of its components) into different eigenstate components of the target wave function. In ${}^1\psi_g(x)$, the main vibrational components are ${}^1\varphi_\upsilon(x)$ with $\upsilon = 7$ to $\upsilon = 11$ so that the population of at least six singlet eigenstates should be transferred to six triplet eigenstates. This transfer is equivalent to a partial mapping of the quantum information of the initial state into the final state. Because the initial state is nonstationary, the phases are dynamically evolving and the possible information content on the relative phases[32,33] cannot be transferred.

To select the components of the target state, one should analyze the Franck−Condon amplitudes of the initial vibrational eigenstates with the set of possible target eigenstates. This map of Franck−Condon amplitudes, F_{ij}, is shown in Figure 7. The choice of target vibrational state will depend on the choice of strategy. In this section, we will discuss parallel transfer of the wave packet, that is, the transfer of all the components at the same time. In the next section, we will consider the sequential transfer of components.

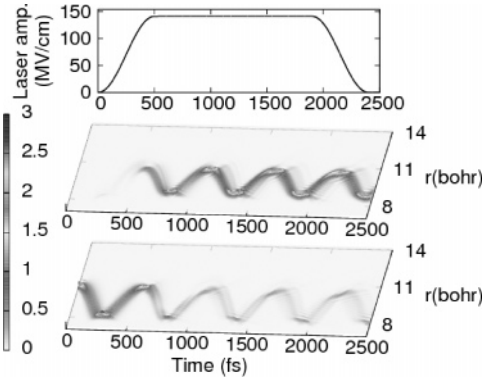

Figure 8. Dynamics of the parallel spin-switch in the coordinate representation. We show the laser shape (top panel) and the target triplet (middle) and initial singlet (bottom) wave packets.

From the perspective of the Franck−Condon map, to achieve the parallel wave packet transfer, the following set of restrictive conditions should be met: First, for each initial and target component of the transfer, the Franck−Condon amplitude should be similar so that the same laser duration τ could be used to maximize the transfer of every component. Second, the energy differences between adjacent initial components and target components (the vibrational quanta) should also be similar so that all transferred initial components are at the same time in resonance with their respective target components. In the coordinate representation, these conditions often imply that the singlet and triplet potentials have similar topologies as in our example. The parallel transfer is straightforward for identical (that is, nondisplaced) potentials.

For the initial wave function in our problem, with $\upsilon = 7$ to $\upsilon = 11$ as important initial eigenstate components, the conditions given by the circles in Figure 7 provide one of the best choices. They imply the switching of ${}^1\varphi_\upsilon(x) \rightarrow {}^3\varphi_{\upsilon'}(x)$ with $\upsilon' = \upsilon - 3$. With $\epsilon = 141.4$ MV/cm (implying a peak intensity of ∼26.6 TW/cm^2), the Stark effect on $V_T(x)$ shifts the potential energy such that ${}^3\Phi_4(x;\epsilon)$ is approximately on resonance with ${}^1\varphi_7(x)$, ${}^3\Phi_8(x;\epsilon)$ is near resonance with ${}^1\varphi_{11}(x)$, and so forth for the remaining vibrational components. Because $F_{\upsilon,\upsilon-3}$ are quite similar for all the υ with important initial populations, in $\tau =$ 1.6 ps, the whole initial wave packet can be transferred toV_T-(x). Figure 8 shows the laser and the dynamics of the wave packet in $V_S(x)$ and $V_T(x)$ in the coordinate representation. The final wave packet is very similar to the first one, but shifted about 3 vibrational quanta to lower energies in $V_T(x)$, as Figure 9 shows.

The maximal efficiency of the overall parallel transfer in this case is 87%. In most cases, it will be difficult to improve this result because perfect population transfer requires almost exact resonant conditions for every component. Because of the differences in the potentials and the anharmonicity of each potential, the energy difference between adjacent states in the initial and target wave packets will not be the same, and no perfect resonance will be achieved with a single amplitude for all the transitions involved. Additionally, the choice of τ cannot maximize the transfer for every component. The parallel transfer is a two-parameter control by which one can only maximize the overall population transfer. However, the advantage of the method is that it is quite less sensitive to pulse amplitude fluctuations. Indeed, for the numerical result just shown, the coupling is larger than the energy spacing between adjacent states (so that each state-to-state transfer in the parallel switch is not independent of the others), but the efficiency of the overall

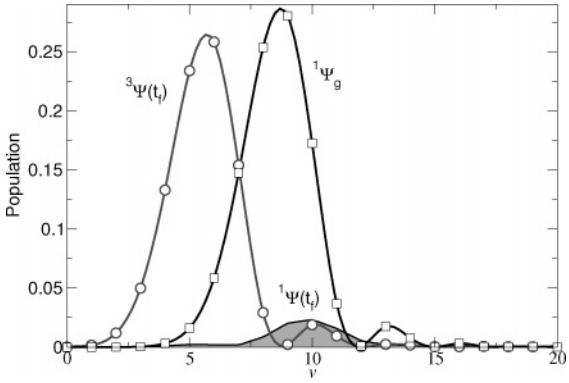

Figure 9. Initial singlet (squares) and final triplet (circles) wave packets in the energy representation (labeled by the vibrational quanta) obtained after the parallel spin-switch scheme. The efficiency of the overall transfer is nearly 90%, and the wave function is shifted to lower energies (3 vibrational quanta) during the transfer. Part of the inital wave packet (shadowed region) remains in $V_S(x)$ at final times.

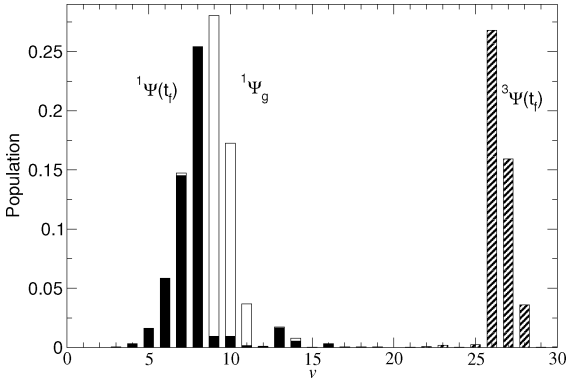

Figure 10. Initial singlet wave packet ($^1\psi_g$) and final mixed-multiplicity wave packet in the energy representation (labeled by the vibrational quanta) achieved after the sequential spin-switch. The solid bars represent the population of the singlet and triplet vibrational components of the final wave packet. The initial components (empty bars) overlap the final components in the singlet region.

transfer is high and can be completed in quite shorter times than those required for other state-selective transitions.

3.3. Sequential Transfer. In this section we will show a different procedure, based on sequential transfer, which allows a higher degree of manipulation at the cost of increasing the experimental needs. The sequential transfer requires finding proper target vibrational states for each selected initial component such that the transfer is selective and independent for each component. In our model, this can be achieved by choosing the target state j for a given initial state i in a region of the potential such that F_{ij} is relatively small for all quantum states around i and j (see the Franck−Condon map of Figure 7) and the anharmonicity is high so that the couplings of the nonselected transitions, $V_{i+n,j+n}$ ($n \neq 0$), are smaller than the energy detuning of each respective transition in the presence of the field, $\Delta E_{i+n,j+n}(\epsilon)$. Then, while the population is switched between $^1\varphi_i(x)$ and $^3\varphi_j(x)$ because $\Delta E_{i,j}(\epsilon) = 0$, the population in all other wave packet components remains unchanged.

As an example of the efficiency of the method, we shall switch the components $v = 9,10,11$ of $^1\psi_g(x)$ to $v = 26,27,28$ in $V_T(x)$, respectively. The Franck−Condon amplitudes of each transition, shown with diamonds in Figure 7 are, respectively, $F_{9,26} = 0.03925$, $F_{10,27} = 0.0505$, and $F_{11,28} = 0.0628$. The sequential transfer is performed by first applying a pulse that shifts $V_T(x)$ (preparing $U_T(x;\epsilon)$), making $^1\varphi_{11}(x)$ on resonance with $^3\Phi_{28}(x;\epsilon)$ and switching the population with $\epsilon = 108.3$ MV/cm and $\tau = 14$ ps, then applying a second pulse that shifts into resonance $^1\varphi_{10}(x)$ with $^3\Phi_{27}(x;\epsilon)$ with $\epsilon = 108.0$ MV/cm and $\tau = 15.5$ ps, and finally applying a third pulse that puts in resonance $^1\varphi_9(x)$ with $^3\Phi_{26}(x;\epsilon)$ by using $\epsilon = 107.7$ MV/cm and $\tau = 20$ ps.

Although each successive pulse in the sequence generates a Stark shift that induces the crossing of the remaining levels to be transferred at the switch on and off, the transitions are approximately independent because the transfer is very sensitive to strict resonance conditions and the pulses can be shaped with fast slopes before and after the plateau region. Therefore, the method is not very sensitive to the pulse order. However, it is convenient to choose a pulse sequence of decreasing pulse amplitudes. Then the pulse acting on the nth transition does not affect any of the previous ones (the induced Stark shift is smaller than what is needed for resonance), and by choosing an adequate time duration, it can maximize the transfer by taking into account the possible flow of population induced by the previous pulses at the switching on and off periods. In Figure 10 we show the initial and final wave packets in the eigenstate representation. The final wave function is a mixed singlet and triplet wave packet where only the chosen populations have been selectively switched to the triplet potential.

The inconvenience of the sequential implementation is its high sensitivity to small variations in the field amplitude. For a single-state switch, the selective transfer required choosing a target state such that the coupling $V_{i,j}$ was smaller than the energy difference between adjacent states, $\Delta\omega \equiv \Delta E_{i,j\pm1}$, that is, essentially the vibrational quanta. However, when initially there are several vibrational states populated, to make the transfer independent for each component, the conditions for the sequential transfer are more demanding. In particular, when a laser is switching the population between $^1\varphi_i$ and $^3\varphi_j$, the remaining components of the wave packet are only slightly off resonance. The detunings, $\Delta E_{i+1,j+1}$ or $\Delta E_{i-1,j-1}$, are either due to the vibrational quanta differing in both singlet and triplet potentials (when $U_S(x)$ and $U_T(x)$ are different) and/or because the potentials are anharmonic (as in our case) since, in general, j is a different vibrational level than i. In either case, the detuning is likely to be quite smaller than the vibrational quanta. For instance, if both potentials are harmonic with the same harmonic frequency, the sequential transfer cannot be achieved because all transitions are exactly on resonance with a single amplitude.

The advantage of the sequential scheme is the higher degree of control that can be achieved since now more lasers and thus more parameters are manipulating the dynamics. In fact, even when the energetics of the system do not allow an independent transfer for each wave packet component, it is in principle possible to find optimal parameters that compensate the interferences at each transition so that the overall sequence maximizes the population transfer for each component. However, finding the optimal pulse parameters in this general case requires the use of a more sophisticated procedure such as a learning algorithm.[34]

4. Applications of the Selective Spin-Switch in Rb_2

The different transfer schemes suggested thus far were based on the possibility of applying a simple extension of the two-level Rabi formula (eq 1) to the strong pulse dynamics. The choice of target state and strategy (selective, parallel, or sequential transfer) was suggested by knowledge of the vibrational eigenstates and the Franck−Condon amplitudes that depended on the molecular model. In this section, we show that the previous strategies can be applied to different scenarios that

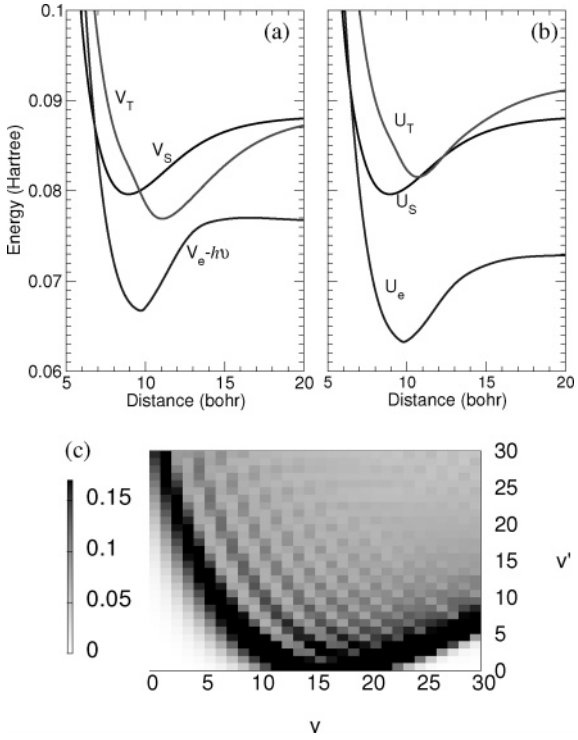

Figure 11. Possible implementation of the NRDSE in Rb_2 between $D^1\Pi_u$ (V_S) and $3^3\Sigma_u$ (V_T) using the auxiliary triplet $5^3\Pi_g$ (V_e) with a laser of carrier frequency $\omega = 8800$ cm^{-1} and $\epsilon \sim 77$ MV/cm (implying a peak intensity of $\sim$7.9 TW/cm^2). (a) Ab initio electronic curves adapted from ref 29. The auxiliary triplet which is used to create the necessary Stark shift is shown with the energy shifted by the laser frequency. (b) LIPs. (c) Franck−Condon map (in gray scale) showing the overlap between vibrational eigenstates of the singlet (υ) and those of the triplet (υ').

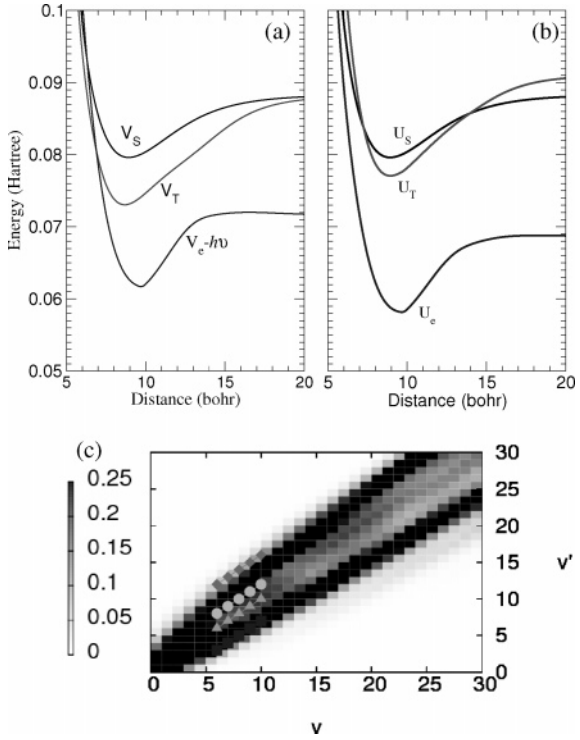

Figure 12. Possible implementation of the NRDSE in Rb_2 between $D^1\Pi_u$ (V_S) and $2^3\Pi_u$ (V_T) using the auxiliary triplet $5^3\Pi_g$ (V_e) with a laser with carrier frequency $\omega = 9900$ cm^{-1} and $\epsilon \sim 77$ MV/cm (implying a peak intensity of $\sim$7.9 TW/cm^2). (a) Ab initio electronic curves adapted from ref 29. The auxiliary triplet, which is used to create the necessary Stark shift, is shown with the energy shifted by the laser frequency. (b) LIPs. (c) Franck−Condon map (in gray scale) showing the overlap between vibrational eigenstates of the singlet (υ) and those of the triplet (υ'). The symbols in the plot show different conditions that imply an overall shift of $\Delta\upsilon = -3,0,2,6$ vibrational quanta (from the crosses to the diamonds, respectively) in the wave packet transfer. For $\Delta\upsilon = 0$ maximum parallel transfer is achieved. The results under these conditions are explored in Figure 13.

occur in molecules. Ultimately, the validity of the schemes relies on the structure of the Franck−Condon maps (as shown in Figure 7), which are rather general, and not on the specific details of the potentials, where the simplifying assumptions of the model (based on identical but displaced Morse potentials) seems more questionable.

To show the possible applications of the previous schemes to a specific molecule, we consider two cases in Rb_2: the transfer of population from the singlet $D^1\Pi_u$ state (V_S) to the triplet $3^3\Sigma_u$ potential (V_T), or from $D^1\Pi_u$ to $2^3\Pi_u$ (V_T). In the first case, we use a laser with carrier wavenumber 8800 cm^{-1} to induce closely off-resonant interaction with the potential $5^3\Pi_g$ (V_e). In the second case, the same $5^3\Pi_g$ potential causes the Stark shift by using a pulse with carrier wavenumber 9900 cm^{-1}.

Figures 11 and 12 show the potential energy curves and Franck−Condon maps obtained for the chosen transitions in Rb_2. The electronic states were obtained by ab initio calculations by Park et al.,[29] whereas the Franck−Condon amplitudes (panel c) were calculated by numerically integrating the overlap integrals of the vibrational eigenstates obtained by the Fourier-grid Hamiltonian technique.[35] In the figures, we also show the triplet light-induced potentials that are formed with $\epsilon = 77$ MV/cm (implying a peak intensity of $\sim$7.9 TW/cm^2, panel b).

As we have explained before, the important parameters to control the spin−orbit coupling are the Franck−Condon amplitudes and the energy difference between the vibrational states in $V_S(x)$ and $V_T(x)$. Comparing Figure 7 of the general model in Section 3 with panel c in Figure 11 for the first application to a Rb_2 transition, we can easily infer that it will not be possible to apply a similar strategy to both cases. The structure of the Franck−Condon maps are very different in the region of the initial wave function (between $\upsilon = 7$ and $\upsilon = 12$ in V_S). While in Figure 7, there are clearly different regions (diamonds and squares) that allow parallel and sequential transfers, in Figure 11, it is not possible to distinguish these regions in the Franck−Condon map. Certainly, it will not be possible to transfer the wave packet in parallel.

The second chosen transition in Rb_2 is a good candidate to apply the proposed schemes, with a Franck−Condon map (panel c in Figure 12) similar to that of the general model (Figure 7). On the other hand, the different vibrational quanta in $V_S(x)$ and $V_T(x)$ (33.4 and 41.8 cm^{-1}, respectively), is quite large. The difference in the vibrational quanta affects the transfer in the same way as the anharmonicity, enabling the sequential transfer (Section 3.3) but reducing the efficiency of the parallel transfer.

We have further estimated the expected maximum yield of spin transfer of $^1\psi_g(x)$ from the $D^1\Pi_u$ to the $2^3\Pi_u$ potentials. Figure 13 shows the maximum population transferred during 20 ps at different laser intensities. At low intensities, we observe clusters of peaks that imply the sequential transfer of adjacent eigenstates of $^1\psi_g(x)$. For instance, at $\epsilon \sim 92.5$ MV/cm (with $\sim$11.4 TW/cm^2 peak intensity), the Stark shift induces the resonance between the $^1\phi_8(x)$ component of the initial wave packet and the target $^3\phi_{14}(x)$ wave function; around this value, the different peaks reflect the transfer of the other vibrational components so that more than 90% of the initial wave function is sequentially transferred to the triplet potential with an energy displacement of approximately 6 vibrational quanta. That is,

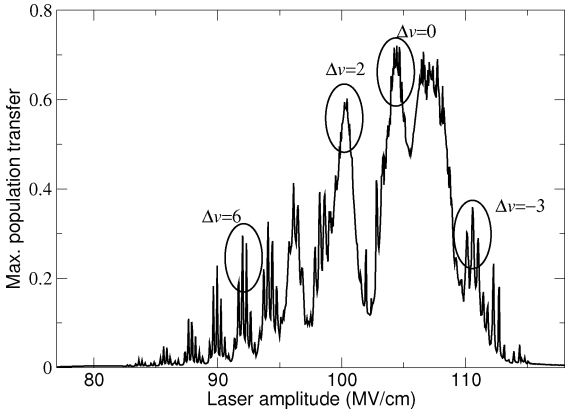

Figure 13. Maximum population transferred from $D^1\Pi_u$ to $2^3\Pi_u$ after 20 ps for different laser amplitudes. With $\epsilon \sim 100$ and $\epsilon \sim 104$ MV/cm, the transfer can proceed in parallel, with an overall shift of $\Delta v = 2$ and 0 vibrational quanta, respectively. Whereas with $\epsilon \sim 92$ and 110 MV/cm, the transfer can proceed sequentially, with an overal shift of $\Delta v = 6$ and -3 vibrational quanta, respectively.

the switching occurs from ${}^1\varphi_v(x) \rightarrow {}^3\varphi_{v'}(x)$ with $v' = v + 6$ ($\Delta v = 6$). The similar cluster structures at moderate intensities show that the initial wave function can be sequentially transferred to different target triplet vibrational states, implying different shifts in the vibrational quanta of the overall wave packet.

However, as the laser intensity increases, the structure of a cluster of distinguishable peaks collapses into a broad band. This fact reflects that the Franck−Condon amplitudes are increasing so that the detuning is not large enough to avoid the transfer of adjacent vibrational components: that is, the transfer is no longer independent for each component. At the highest value (for $\epsilon \sim 103.8$ MV/cm), the overall population transferred is ∼70%. This is the highest efficiency that one can achieve by parallel transfer of ${}^1\psi_g(x)$ from $D^1\Pi_u$ to $2^3\Pi_u$. At this amplitude, $U_S(x)$ is practically in resonance with $U_T(x)$ and the spin switch involves no energy shift in the transfer of ${}^1\psi_g(x)$ ($\Delta v = 0$). Finally, at larger pulse intensities, the Franck−Condon amplitudes decrease again and some partial sequential transfer can be again achieved, but with lower efficiency. Additionally, since $U_S(x)$ is now below $U_T(x)$, the vibrational displacement in the transfer involves a negative Δv, and some components of the initial wave packet cannot be transferred.

5. Conclusions

The numerical results presented in this work, both for the general simple model and for the implementation in Rb_2, show that it is in principle possible to achieve vibrationally selective population transfer between electronic states of different multiplicity by using strong nonresonant pulses. Quantum state selectivity imposes very restrictive conditions on the required laser fields. First, the target state should be chosen appropriately so that the generalized Rabi formula applies to the population transfer. Second, the population switch can proceed either in parallel or sequentially. In the first case, from the perspective of optimal control, the dynamics is not fully controllable. The maximum yields that can be achieved depend crucially on the molecular system. In the second case, on the contrary, the dynamics can in principle be controlled. However, the experimental needs on the laser pulses are much more demanding in the later case. The conditions required for the schemes to optimally perform are still far from what can be achieved with current technology. One needs to reduce the pulse intensity and pulse duration requirements of the schemes before an experimental test of the scheme is feasible, particularly to reduce the role of multiphoton ionization of the molecule.

The intensity requirements are given by the need of strong Stark shifts. If $V_T(x)$ is closer to $V_S(x)$, then one will need less intense pulses. Additionally, one can tune the laser frequency closer to resonance between $V_T(x)$ and $V_e(x)$. Then the Stark shift will depend quasilinearly on ϵ instead of quadratically (eq 3). However, this will make more difficult the adiabaticity of the population transfer to a single vibronic triplet state because more population will temporally excite $V_e(x)$, and additionally, the state-selective transfer will be more sensitive to instabilities in the energy of the field. For other singlet−triplet transitions in Rb_2, it might be possible to reduce the laser intensity needs to one-half or one-quarter of those used here.

The time needed for the spin switch depends inversely on the spin−orbit coupling (eq 6) so that, for larger V_{SO}, one could reduce the laser duration. However, in order to guarantee state-to-state selectivity, the target state (and thus F_{ij}) must be chosen so that the final time is solely fixed by the vibrational energy structure of the initial singlet and target triplet wave packets. The time constraints are given by the energy difference between adjacent vibrational states (in the state-to-state selective transfer) or, even worse, by the energy difference between the vibrational quanta in the singlet and triplet potentials (in the sequential transfer). For Rb_2, these constraints will put the time duration of the spin switch in the 10−20 ps regime. Only in the parallel transfer one might be able to use femtosecond laser pulses.

Other than disregarding multiphoton ionization and assuming the molecular alignment with the field, which may hamper or make difficult the success of the experiment, it is the laser stability requirements of the field that will really affect the outcome of the state-selective spin transfer. Using the simple model of Section 3, we have observed that one needs a laser stability in the pulse amplitude quite better than 2% in order to ensure the state selectivity in the sequential transfer. This can also be inferred from Figure 13. Small variations in the field amplitude lead to different resonances (different spikes in the maximum population transfer in Figure 13). However, the stability is much larger in the region of parallel transfer. Although the fidelity of the transfer and the degree of quantum control are weaker in the parallel scheme, we expect this strategy to be ready for experimental test with available laser facilities.

Acknowledgment. Financial support from the Dirección General de Investigación of Spain under project no. CTQ2005-04430 is acknowledged. J.G.-V. also thanks the Spanish Ministry of Education and Science for an FPI Grant.

References and Notes

(1) Rice, S. R.; M. Zhao, M. *Optical Control of Molecular Dynamics*; Wiley: New York, 2000.
(2) Brumer, P.; Shapiro, M. *Principles of the Quantum Control of Molecular Processes*; Wiley: New York, 2003.
(3) Lefebvre-Brion, H.; Field, R. W. *The Spectra and Dynamics of Diatomic Molecules*; Elsevier: Amsterdam, 2004.
(4) Zhang, B.; Berg, L.-E.; Hansson, T. *Chem. Phys. Lett.* **2000**, *325*, 577.
(5) Zhang, B.; Gador, N.; Hansson, T. *Phys. Rev. Lett.* **2003**, *91*, 173006.
(6) Merchán, M.; Serrano-Andrés, L.; Robb, M. A.; Blancafort, L. *J. Am. Chem. Soc.* **2005**, *127*, 1820.
(7) *The Physics of Quantum Information*; Bouwmeester, D., Ekert, A., Zeilinger, A., Eds.; Springer-Verlag: Berlin, 2000.
(8) Nielsen, M. A.; Chuang, I. L. *Quantum Computation and Quantum Information*; Cambridge University Press: Cambridge, 2000.
(9) Hübner, W.; Zhang, G. P. *Phys. Rev. B* **1998**, *58*, 5920(R).
(10) Zhang, G. P.; Hübner, W. *Phys. Rev. Lett.* **2000**, *85*, 3025.
(11) Gómez-Abal, R.; Hübner, W. *Phys. Rev. B* **2002**, *65*, 195114.

(12) Gómez-Abal, R.; Hübner, W. *J. Phys.: Condens. Matter* **2003**, *15*, S709.

(13) Gómez-Abal, R.; Ney, O.; Satitkovitchai, K.; Hübner, W. *Phys. Rev. Lett.* **2004**, *92*, 227402.

(14) Satitkovitchai, K.; Pavlyukh, Y.; Hübner, W. *Phys. Rev. B* **2005**, *72*, 045116.

(15) Korolkov, M. V.; Schmidt, B. *Chem. Phys. Lett.* **2002**, *361*, 432.

(16) Korolkov, M. V.; Manz, J. *J. Chem. Phys.* **2004**, *120*, 11522.

(17) Sussman, B. J.; Ivanov, M. Y.; Stolow, A. *Phys. Rev. A* **2005**, *71*, 051401(R).

(18) Sussman, B. J.; Townsend, D.; Ivanov, M. Y.; Stolow, A. *Science* **2006**, *314*, 278.

(19) Chan, C. K.; Brumer, P.; Shapiro, M. *J. Chem. Phys.* **1991**, *94*, 2688.

(20) Sola, I. R.; González-Vázquez, J.; Malinovsky, V. S. *Phys. Rev. A* **2006**, *74*, 043418.

(21) González-Vázquez, J.; Sola, I. R.; Santamaria, J.; Malinovsky, V. S. *J. Chem. Phys.* **2006**, *125*, 124315.

(22) González-Vázquez, J.; Sola, I. R.; Santamaria, J.; Malinovsky, V. S. *Chem. Phys. Lett.* **2006**, *431*, 231.

(23) Bandrauk, A. D.; Sink, M. L. *Chem. Phys. Lett.* **1978**, *57*, 569.

(24) Shore, B. W. *Theory of Coherent Atomic Excitation*; Wiley: New York, 1990.

(25) Frohnmeyer, T.; Hofmann, M.; Strehle, M.; Baumert, T. *Chem. Phys. Lett.* **1999**, *312*, 447.

(26) Bandrauk, A. D.; Aubanel, E. E.; Gauthier, J.-M. In *Molecules in Laser Fields*; Bandrauk, A. D., Ed.; Dekker: New York, 1994.

(27) In this equation, we are using as a ket (or bra) the vector that has as components the wave packets in each potential. Thus $|^3\Phi_j\rangle$ is the column vector that has $^3\Phi_j(x)$ as the component in the $U_T(x)$ potential and zero as components in the other LIPs. $\mathscr{R}$ is the transformation from the adiabatic to the diabatic basis. The approximate sign in the equation is due to the fact that $\mathscr{R}$ was defined previously to diagonalize $\mathscr{V}$ and not the full diabatic Hamiltonian, $\mathscr{H}_{\text{diab}} = \mathscr{T} + \mathscr{V}$, for numerical simplicity. However, one could obtain an $\mathscr{R}'$ that diagonalizes $\mathscr{H}_{\text{diab}}$ for which $V_{ij} = U_{ij}$.

(28) Gador, N.; Zhang, B.; Andersson, R.; Johansson, P.; Hansson, T. *Chem. Phys. Lett.* **2003**, *368*, 202.

(29) Park, S. J.; Suh, S. W.; Lee, Y. S.; Jeung, G.-H. *J. Mol. Spectrosc.* **2001**, *207*, 129.

(30) Kosloff, R. *Annu. Rev. Phys. Chem.* **1994**, *45*, 145.

(31) Scrinzi, A.; Ivanov, M. Yu.; Kienberger, R.; Villeneuve, D. M. *J. Phys. B* **2006**, *39*, R1.

(32) Weinacht, T. C.; Ahn, J.; Bucksbaum, P. H. *Phys. Rev. Lett.* **1998**, *80*, 5508.

(33) Ahn, J.; Weinacht, T. C.; Bucksbaum, P. H. *Science* **2000**, *287*, 463.

(34) Judson, R. S.; Rabitz, H. *Phys. Rev. Lett.* **1992**, *68*, 1500.

(35) Marston, C. C.; Balint-Kurti, G. G. *J. Chem. Phys* **1989**, *91*, 3571.